Robotica (1998) volume 16, pp. 543–550. © 1998 Cambridge University Press

A compliant controller dynamically updating the compliance center by contact localization

Sungchul Kang,* Yong K. Hwang,† Munsang Kim,* Chongwon Lee* and Kyo-Il Lee‡

(Received in Final Form: October 14, 1997)

SUMMARY

This paper presents a compliant control method for insertion of complex objects with concavities. Most work on robot assembly using compliant motion control schemes focuses on overcoming jamming conditions for simple peg-in-hole problems, and cannot be used for complex shapes frequently encountered in assembly applications. When an object is being inserted to a hole or slot with a small clearance, a contact path is issued to compensate for uncertainties. When the object shape is complex, however, the contact state changes several times and severely, making compliant control difficult. The algorithm presented here is capable of generating satisfactory compliant motion control in spite of changing contact states. During the execution of a nominal motion plan, it computes the actual position of the contact point from the force/torque sensor reading using a contact localization algorithm. It then dynamically updates the center for compliance to the computed contact point, and minimize the chance of jamming and unwanted collisions. The control scheme has been implemented on hardware and tested on the task of inserting a T-shape into a C-shape involving a very tight tolerance. The insertion motion was accomplished by a sequence of 2 translational and 1 rotational compliant motions, and successfully executed by the proposed compliant motion controller.

KEYWORDS: Compliant motion; Motion planning; Insertion; Concave object; Contact; Planar robot; Contact localization; Stiffness control; Moving compliance frame; Real-time controller.

I. INTRODUCTION

Most research efforts on robot assembly using compliant motion control schemes[1, 2] have focused on assembling objects having a simple geometry, e.g., peg-in-hole or electronic components and on overcoming jamming due to robot positioning errors or uncertain environments by correcting an insertion path using contact force/torque information.[3, 4] Recently, various robot applications, e.g., assembly by mobile robots, teleoperation and robotic surgery, require an insertion of a complicated object into an uncertain environment. In these applications, the size of the entry hole is often smaller than some dimension of the peg, and multi-step compliant motions are required for insertion rather than a single motion. Even though there might be a non-contact insertion path, a contact path is often easier to execute. To meet these needs, an insertion technique which plans a contact path and executes a compliant motion needs to be developed to complement human skills and increase the autonomy of robotic systems.

This paper presents a control algorithm for insertion operations involving complex objects and multi-step compliant motions, and describes an on-going work on compliant motion planning. The compliant motion control of a complex object is difficult for two reasons. First, there are many more contact states than a simple peg-in-hole, and results in frequent contact state changes. Second, the magnitude of the changes, e.g. the distance between the new and previous contact points can be quite large, requiring the controller to reset the center of compliance. The key feature of the proposed compliant motion controller is 1) dynamic on-line sensing and computation of the contact point based on the readings from the wrist force/torque sensor, and 2) subsequent updating of the center of compliance to minimize jamming and undesired collisions. Another contribution is the extension of the contact localization algorithm to rectangular objects. For planning of compliant motions, we are developing an algorithm based on the skeleton refining approach,[5, 6] since the more rigorous backprojection method[7] has a high complexity, especially for complex objects requiring multi-step motions.

This paper is organized as follows. Section II reviews the previous work done on compliant motion planning and control. Next, a complex insertion task is introduced and used to illustrate our algorithm. Section IV presents the compliant motion control algorithm, and hardware experimental results are presented in Section V. The work on planning is described next, and finally, conclusions and future work are discussed in Section VII.

II. PREVIOUS WORK

Numerous results are available on both planning and control of motions under uncertainties. Planning is concerned with computing a nominal compliant motion from the robot controller model, object models and their associated

* Humanoid Robot Research Center, KAIST, P.O. Box 131, Cheongryang, Seoul, (South Korea)
E-mail:kasch@kistmail.kist.re.kr
† Intelligent System Principles Dept. 9621, Sandia National Laboratories, MS 1008, P.O. Box 5800, Albuquerque, N.M. 87185 (USA) E-mail:hwang@isrc.sandia.gov
‡ Dept. Mech. Design & Prod. Engineering, Seoul National University, 56-1, Shinlim-dong San, Kwanak-gu, Seoul (South Korea) E-mail:ki@plaza.snu.ac.kr

https://doi.org/10.1017/S0263574798000058 Published online by Cambridge University Press

uncertainties, while control algorithms are aimed at executing the planned motion in spite of uncertainties such as friction, control and sensing errors.

Compliant motion can be achieved by either controlling the joint torques or by controlling the position command to a position-controlled manipulator. In the first approach, such as in stiffness control[2] or impedance control,[8] the desired stiffness or impedance can be obtained by controlling the joint torques during execution of a constrained motion. The controller is responsible for computing required joint torques to achieve a desired behavior. In the second approach,[1,4] robot compliance is achieved by controlling the command trajectory. An external positional feedback loop is typically required. There is a somewhat different type of control scheme called the hybrid position/force control.[9] It is motivated by the natural and the artificial constraints, and is aimed at tracking both the desired position and the force trajectory using the orthogonality (or reciprocality) between the position direction and the force direction to be controlled. Since compliant motions in assembly are usually required to be slow to avoid impact and need not follow force trajectories exactly, it is appropriate to adopt stiffness control which assumes a quasi-static motion rather than impedance control or hybrid position/force control.

There is an extensive work on contact analysis of the peg-in-hole problem. Vukobratovic and Stokic[10] enumerated all possible contact states for this problem, and presented the conditions for jamming explicitly. Asada and Hirai[11] developed a method to compute feasible motions for multiple-contact cases, and applied it to the peg-in-hole problem using polyhedral convex cones. It is used in assembly planning for computing feasible differential motion directions. As far as planning an insertion motion, Strip[12] has proposed an oriented insertion technique by doing a contact analysis of various convex and star-shaped pegs using friction cones. More recently, Astuti and McCarragher[13, 14] has presented a discrete event controller imitating human decision making mechanism for dual-peg and two-tied peg insertion tasks. The transition among different contact states are modeled as a Markov process and a probabilistic controller has been developed.

Most existing results including the ones mentioned above are limited to insertion tasks involving prismatic objects moving along a 1-dimensional insertion path normal to the mating face. These tasks have the property that the cross section of the object being inserted is a subset of that of the hole or slot. In contrast, our insertion task involves a concave polyhedral peg and hole, and the number of contact states is dramatically increased (approximately quadratic in the number of convex subparts), posing a difficulty for the existing algorithms.

Localization methods of the contact point using force/torque information during insertion have been presented by Zhou, Shi and Li[15] and Tsujimure and Yabuta[16] The coordinates of the contact point are computed by intersecting object surface with the line representing the relationship between the sensed force and torque. When the contact point can be localized on-line, the compliance frame (or the center of compliance) and other control gain parameters can be adjusted dynamically during insertion to improve the controller performance. For example, a stiffness gain can be updated by considering the moving direction and the constraint direction with respect to the compliance frame corresponding to the contact point. In fact, this is one of the key features of our algorithm.

A seminal work on compliant motion planning is presented by Lozano-Perez, Mason and Taylor[7]), where the concept of uncertainty cones is introduced and used to develop a planning methodology called *backprojection*. In this paradigm, motion is planned backward from the goal region toward the start point. For a given goal region, the uncertainty cone is used to compute a *pre-image* such that if the robot starts in the pre-image, it is guaranteed to reach the goal region. This computation is recursively done until the start point is included in one of the pre-images. The notions of goal recognizability and termination conditions are also important in compliant motion planning since the robot joint encoder readings alone cannot tell whether the goal is reached and when to stop motion commands. A number of results[17] have followed, and the current status can be summarized as 1) the complexity of motion planning under uncertainty is exponential in the number of backprojection steps,[18] 2) the backprojection regions are not unique and dependent on the termination condition,[19] and 3) implementation is very difficult beyond 4 dimensions.[20] Most of these methods assume that the positional accuracy degrades as the travel distance increases. We have observed that for a manipulator with a fixed base, the positional error can be bounded independently of the travel distance. We use this observation to develop a more efficient compliant motion planner, and it is discussed in Section VI.

III. TASK ANALYSIS

For the remainder of this paper, the task of inserting a T-shaped object into a C-shaped slot is used to describe the compliant motion control algorithm and conduct a hardware experiment. The concavities of the T shape is used to insert it into a C shape whose slot width is smaller than the width of the T. It is a 3 degree of freedom problem, 2 for translation and 1 for rotation. This example has been inspired by an experiment that make a blindfold human

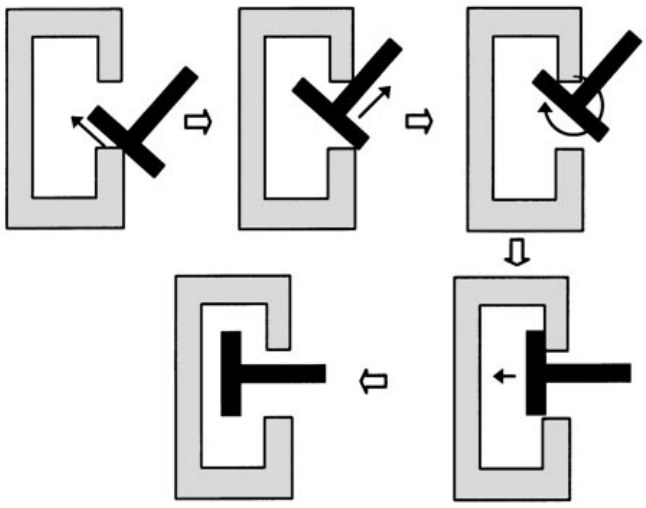


Fig. 1. Insertion sequence for T-shaped object.

https://doi.org/10.1017/S0263574798000058 Published online by Cambridge University Press

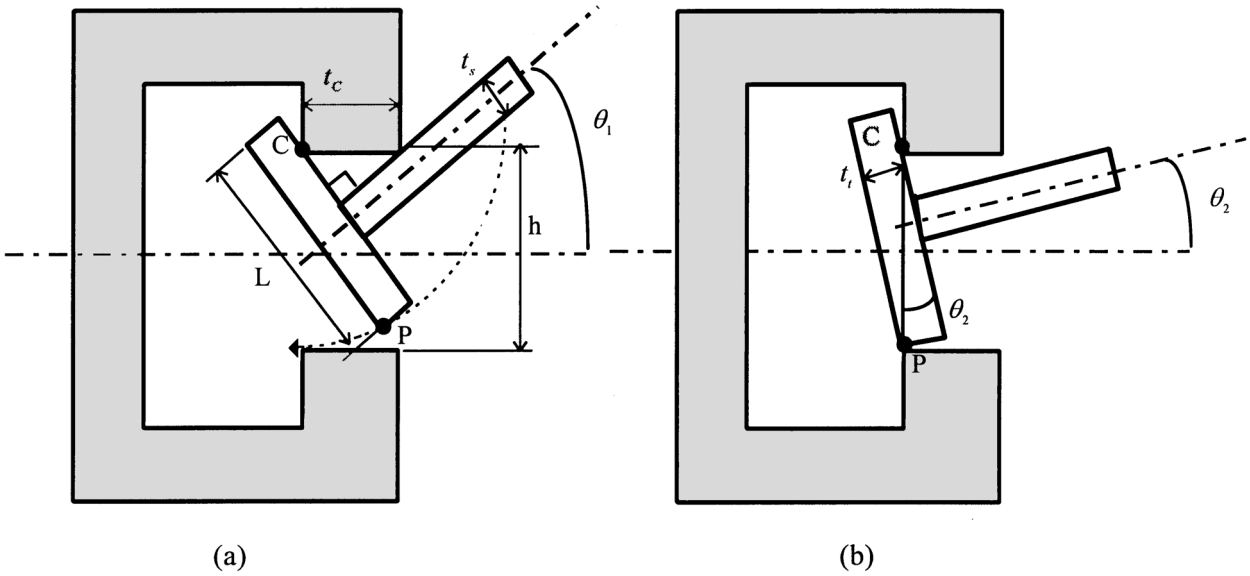


Fig. 2. Insertion conditions when rotating about C.
(a) Configuration of T before rotation
(b) Configuration of T with two contacts

insert a T into a C-shaped slot.[21] A simple path for T insertion in our work has been obtained from the experimental result from a blindfold human. Alternatively, we are developing a motion planner to compute this path automatically (see Section VI).

When a blindfold man inserts T into C with a small clearance, he usually intends to insert it using contacts since an inserting path allowing contacts is simple to be generated and does not require fine position control. Fig. 1 shows a simplified insertion path observed from human T-insertion.

The dimensions of T and C-slot are determined so at least one compliant motion has to be used to accomplish the insertion. As shown in Fig. 2(a), the geometric relation between L, the length of T, and h, the length of the entrance of C, has been derived. Assuming a fixed approach angle θ_1, the maximum length of $\overline{CP}$ is

$$\overline{CP} = \sqrt{\left(t_C \sin\theta_1 + \tfrac{1}{2}t_s + \frac{L}{2}\right)^2 + t_t^2}. \quad (1)$$

When T has been rotated from θ_1 to θ_2 about contact point C, from the relation that $\overline{CP} = h$ in Fig. 2 (b), the maximum length of the L is described as

$$L_{\max} = 2\,(\sqrt{h^2 - t_t^2}) - t_C \sin\theta_1 - \tfrac{1}{2}t_s). \quad (2)$$

Fig. 3 shows a kinematic simulation in IGRIP (Interactive Graphic Robot Instruction Program) to verify the geometrical result of the task analysis for T-insertion.

IV. COMPLIANT MOTION CONTROLLER DESIGN

The compliant controller performs three processes: contact position sensing, compliance frame updating and compliant control that incorporates the above two processes. We first describe the advantages of updating the compliance frame during motion execution.

IV.1. Compliance frame updating

Compliant motion control schemes including Cartesian stiffness control[2, 22] used in this paper maintain a desired stiffness at the compliance frame, which is typically set to the point of the object in robot's hand that makes contact with other object in the work space. During an insertion task, if the contact point moves by a large amount on the surface of the object being inserted, it is necessary to move the compliance frame so it coincides with the contact point. It is especially true for tasks involving large or complex objects. When the contact point has been translated or rotated to another one on the object surface, the stiffness gain should be adjusted to the coordinates of the compliance frame corresponding to the current contact location. If the compliance frame is set to an arbitrary fixed point on the object surface regardless of the contact point, some problems may occur depending on the location of the contact point and the geometry of the object as follows. As shown in Fig. 4(a), if T rotates about a fixed end-point O and not about the contact point C, it may exert a large

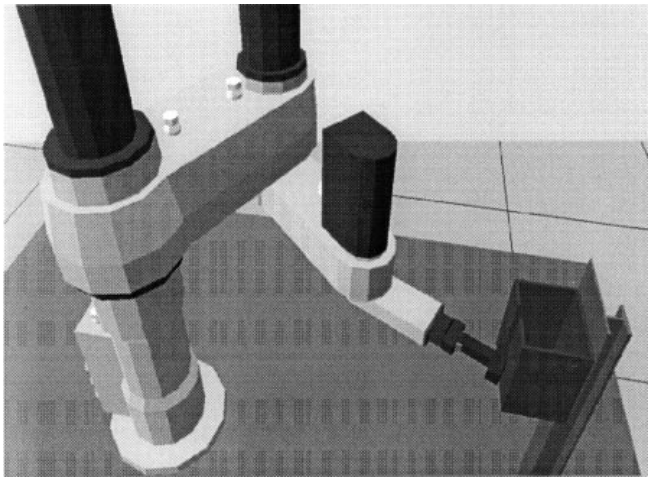


Fig. 3. Kinematic simulation of T-insertion.

https://doi.org/10.1017/S0263574798000058 Published online by Cambridge University Press

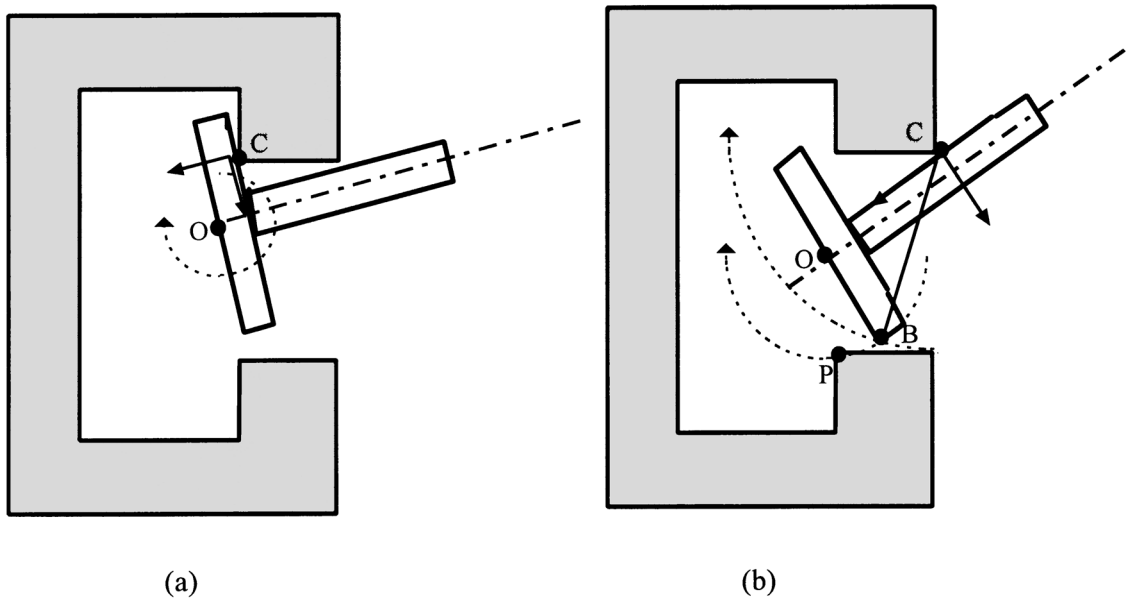


Fig. 4. Problems when rotating about non-contact point O.
(a) Large contact force at C
(b) Collision near P

undesirable force at C resulting in a positional error for O. Another reason to rotate an object about the contact point is shown in Fig. 4(b). The success of an insertion process depends on whether the T shape can pass through the smallest portion of the C slot. A good strategy to use for this is to move the T all the way to one side of the slot, and rotate it against the contact point. In Fig. 4(b) rotation about C has a smaller chance of hitting the lower part of the C slot than rotating about O.

IV.2. Contact localization

To locate a compliance frame to the current contact point during insertion, the location of the contact point should be determined with respect to hand frame or F/T sensor frame. Though the locations of the contact points might be estimated geometrically in the path planning stage, they may not be accurate due to various control errors during insertion. There are on-line contact-point localization algorithms developed based on F/T sensors or tactile sensors. In the case of a task where the contact point is on the object in the robot's hand rather than on the robot hand, a F/T sensor attached to the hand frame has to be used rather than tactile sensor array. Zhou, Shi and Li[15] presented a method to localize a contact point of a tool whose shape is cylindrical or spherical. Generally, the location of the contact point can be determined uniquely from the sensed contact force and moment, F alone. The geometric constraint $\varphi(r)=0$ describing the surface of the tool has to be imposed to get a finite number of solutions. Let Γ be the relation between the contact position vector r and the contact force F,

$$r=\Gamma(F, \varphi). \tag{3}$$

Since the T shape consists of two rectangular blocks, the contact localization algorithm is extended to rectangular shapes. Furthermore, since the T moves in the (X, Y, α) space, it always makes a plane-edge contact where the edge is vertical. An equivalent contact point is defined as the average of all contact points, which is the mid-point of the plane-edge contact shown in Fig. 5. In each of the 5 stages of the insertion operation in Fig. 1, only one contact exists except for the third stage. Since the thickness of the C-shape is small, the two point contact can also be considered as a single point contact. It is also obvious at each stage which of the two rectangular blocks of the T shape makes a contact with C shape.

As mentioned above, the location of the equivalent contact point $r=(r_x, r_y, r_z)$ can be determined as follows using the sensed forces $f_s=(f_x, f_y, f_z)$, the sensed torques $\tau_s=(\tau_x, \tau_y, \tau_z)$ from F/T sensor and the geometric constraint of the rectangular cross section of T. The relation between the resultant force F acting on the equivalent contact point and the measured F/T sensor data (f_s, τ_s) is

$$f_s=F \tag{4}$$

and

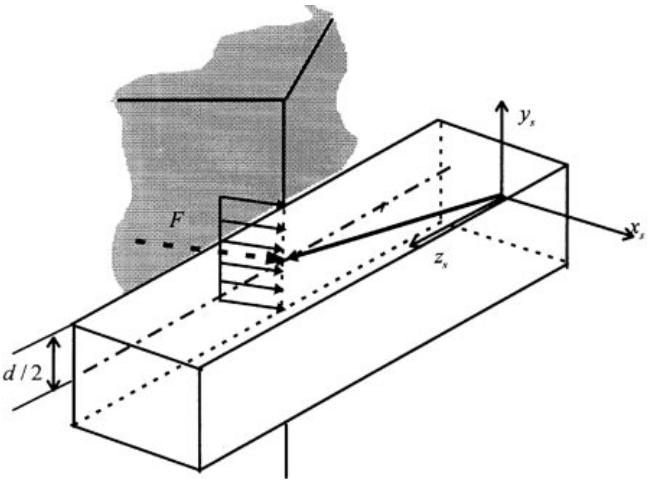


Fig. 5. Estimation of equivalent contact position r by resultant contact force.

https://doi.org/10.1017/S0263574798000058 Published online by Cambridge University Press

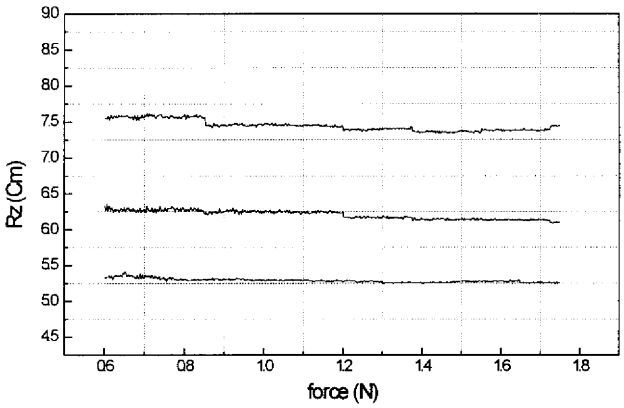


Fig. 6. The results fo contact localization.

$$\tau_s = r \times f_s. \tag{5}$$

Equation (5) can be rewritten as a matrix equation using a skew symmetric matrix $\hat{f}_s$,

$$\tau_s = \hat{f}_s r \tag{6}$$

where

$$\hat{f}_s = \begin{bmatrix} 0 & -f_z & f_y \\ f_z & 0 & -f_x \\ -f_y & f_x & 0 \end{bmatrix}.$$

A unique solution cannot be determined from (6) because the rank ($\hat{f}_s$) is always 2. Thus considering the geometry of the rectangular cross-section of T and the planar motion for T insertion, r can be determined as

$$r_s = \begin{cases} -t_s/2 & \text{if } f_s > 0 \\ t_s/2 & \text{if } f_x < 0, \end{cases} \tag{7}$$

$$r_y = 0 \tag{8}$$

$$r_z = \frac{\tau_y + f_z r_s}{f_x}. \tag{9}$$

The sign of r_s can be found from the sign of f_x as in (7). The computed distance r_z from measured forces and torques is shown in Fig. 6. The cut-off frequency of low-pass filter in F/T sensor was set to 125 Hz. The threshold force that produces a meaningful distance value is about 0.6 N. After the experiments for various distances, 52.5, 62.5 and 72.5 mm, the maximum error is around 2.5 mm—it is due to flexibility in the object, holder and F/T sensor. The computed contact position vector r is then used in real-time to modify both the forward kinematic function and Jacobian which use r as the last link dimension during insertion.

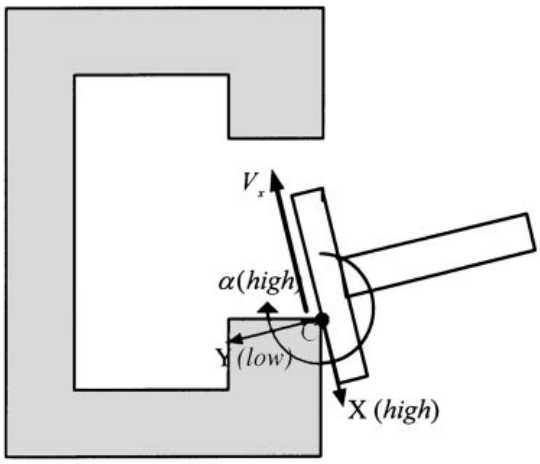


Fig. 7. Stiffness design using compliance frame.

IV.3. Controller design

The compliant motion controller implemented for T insertion is based on the Cartesian stiffness control. It can also be used as a high stiffness PD-type position controller for free space motion since they are the same in structure except the stiffness gain. The control law for free space motion is

$$\tau = {}^{t}J^{T}[{}^{t}K_d({}^{t}X_d - {}^{t}X) - {}^{t}B_d^{t}\dot{X}] \tag{10}$$

where ${}^{t}X_d$, ${}^{t}X$, ${}^{t}\dot{X}$ and ${}^{t}J^{T}$ are the desired trajectory, actual feedback trajectory, actual feedback velocity and transposed Jacobian with respect to the tool frame, respectively. ${}^{t}K_d$ and ${}^{t}B_d$ are the high stiffness proportional gain and the derivative gain with respect to the tool frame, respectively.

In compliant motion, the desired stiffness *Kd* and the desired damping *Bd* is designed with respect to the compliance frame at the contact point. The control law including force feedback is

$$\delta\tau = {}^{C}J^{T}[{}^{C}K_d({}^{C}X_d - {}^{C}X) - {}^{C}B_d{}^{C}\dot{X} - {}^{C}F] \tag{11}$$

where ${}^{C}X_d$, ${}^{C}X$, ${}^{C}J^{T}$ and sensed force ${}^{C}F$ are expressed with respect to the compliance frame at the contact point. The

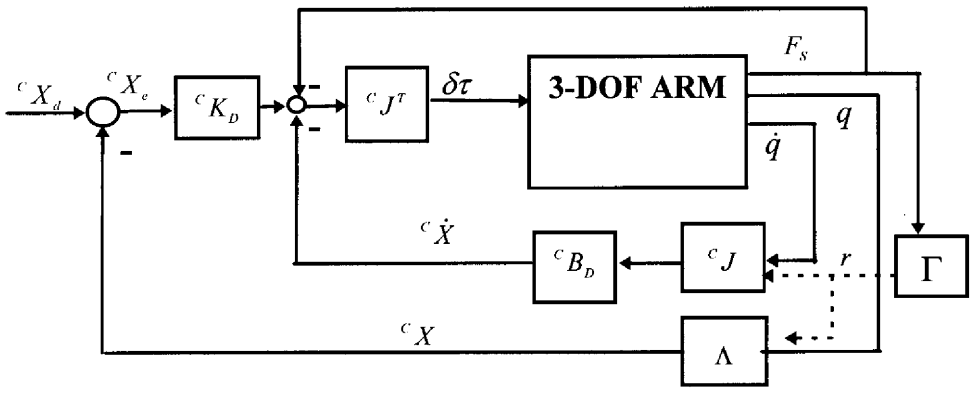


Fig. 8. Block diagram of compliant motion control system.

https://doi.org/10.1017/S0263574798000058 Published online by Cambridge University Press

force feedback loop using ${}^{C}F$ has been added to compensate for the uncertainty in stiffness caused by a rough surface of the environment.

In designing the desired stiffness ${}^{C}k_s$, ${}^{C}k_y$, ${}^{C}k_\alpha$ of the diagonal matrix ${}^{C}K_d$, a low stiffness is set to the direction having a motion constraint while high stiffness is set to the direction of the commanded motion. On the other hand, the low stiffness in the constrained direction can be set to the ratio of tolerable contact force F_{tol} to tolerable position error X_{tol}.[8] For the situation shown in Fig. 7, high stiffness gains are set for X and α direction while a low stiffness is set for Y direction of the compliance frame. Thus the desired stiffness matrix can be set to

$$ {}^{C}K_d = \begin{bmatrix} k_x & 0 & 0 \\ 0 & F_{tol}/y_{tol} & 0 \\ 0 & 0 & k_\alpha \end{bmatrix}. $$

To make the closed loop dynamics have a critically damped response, assuming the inertia matrix be identity for a quasi-static motion, the desired damping matrix B_d can be set to

$$ {}^{C}B_d = 2\sqrt{{}^{C}K_d}. \tag{13} $$

To maintain the compliance frame at the contact point in the compliant motion control during insertion, the last link parameter in the forward kinematics $\Lambda(q, r)$ and Jacobian ${}^{C}J(q, r)$ are updated using r computed from (7), (8) and (9). The block diagram of the compliant motion control for T insertion is shown in Fig. 8.

V. IMPLEMENTATION AND EXPERIMENT

A VME-bus based robot control system, as shown in Fig. 9, which runs in real time OS (VxWorks) has been developed to implement the T insertion. To share the computational loads, a KVME040 CPU board performs the computation for trajectory planning and contact-point localization using JR3 F/T sensor feedback, while a TMS320C30 DSP board handles the computation for stiffness control. The interface between CPU board and DSP board is done by a dual-port RAM to minimize the communication time. This hardware architecture has achieved the trajectory update rate of 200 Hz and feedback servo rate of 1000 Hz.

The robot used in the T insertion is Goldstart GHR350-II SCARA robot which is similar to an Adept robot. To make the robot move in X, Y and α direction in task coordinates for T insertion, it has been reconstructed to a 3-DOF by freezing the third prismatic joint. The T-insertion robot control system and T-insertion are shown in Fig. 10.

In the T insertion experiment, a nominal insertion path has been planned to have the contact between T and C occur at only one point to simplify the algorithm for contact point localization and to avoid jamming. The nominal insertion path ${}^{O}X_d$ is expressed by the trajectory of the point O defined in Fig. 4(a) with respect to robot's base frame. Using the information of the contact location, ${}^{O}X_d$ is modified to ${}^{C}X_d$ on-line. The total insertion time was set to 50 sec. The actual Cartesian trajectories from T insertion is shown in Fig. 11. At the 4th stage in Fig. 11, the T rotates to enter the slot. There are some offsets between the desired path and actual path to ensure contacts in insertion. The measured forces Fx, Fy with respect to the compliance frame is shown in Fig. 12. The forces are controlled to a proper bound to maintain the force tolerance (5 kgf) by the stiffness controller with force feedback.

VI. COMPLIANT MOTION PLANNING

Compliant motion planning has a high complexity in the number of motion steps.[18] Insertion of complex shapes requires multi-step compliant motions, and is likely to require a long computation time. In addition, the implementation is difficult when rotational motion is included. On the other hand, existing gross, i.e., non-contact motion

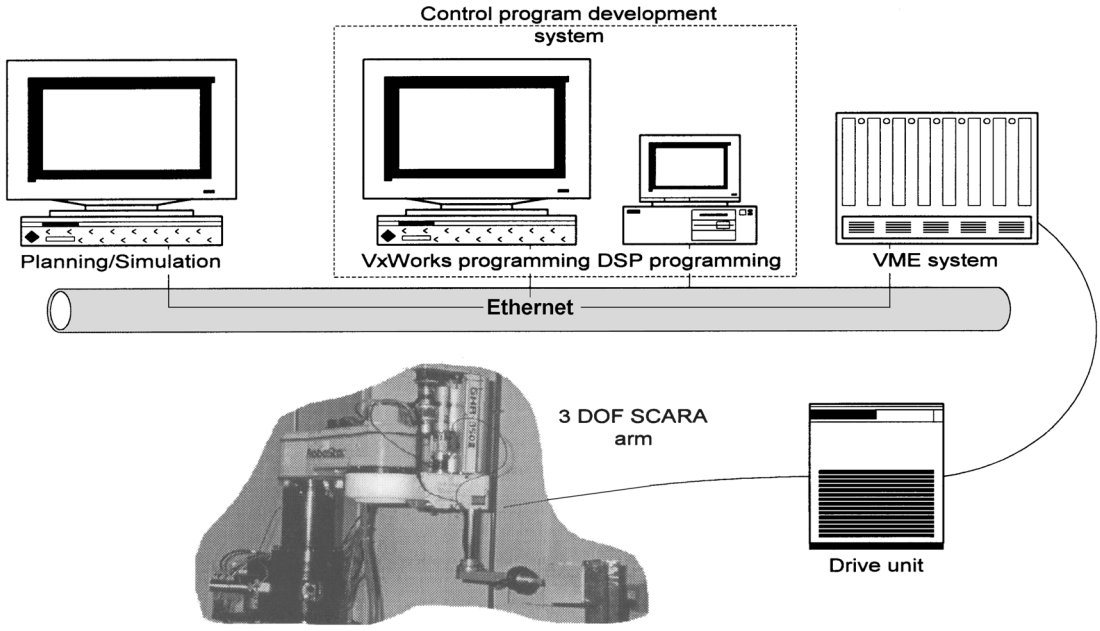


Fig. 9. VME-based real-time control system.

https://doi.org/10.1017/S0263574798000058 Published online by Cambridge University Press

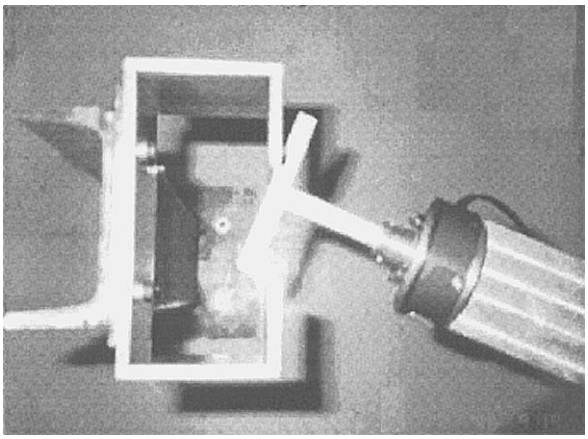


Fig. 10. T insertion experiment.

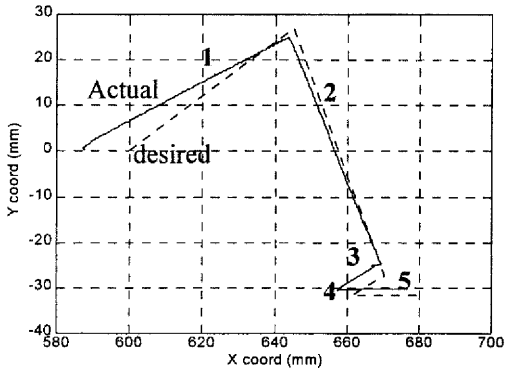


Fig. 11. Command and actual trajectory of the end-point of T insertion.

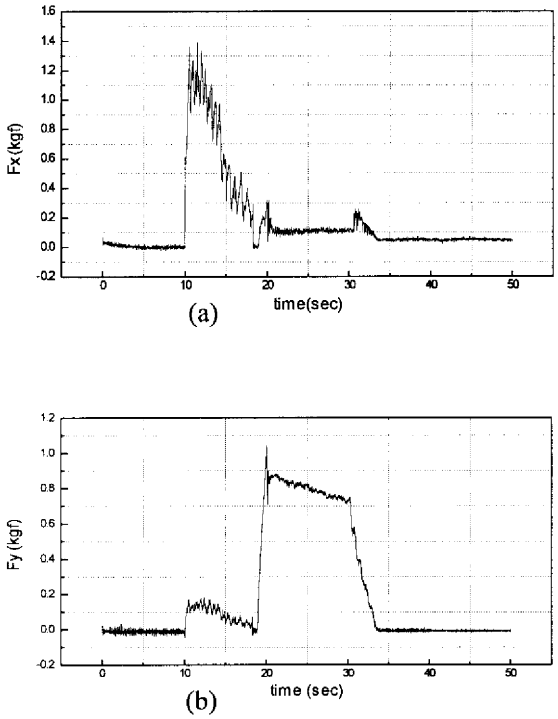


Fig. 12. Measured forces *Fx* (a), *Fy* (b) in T insertion.

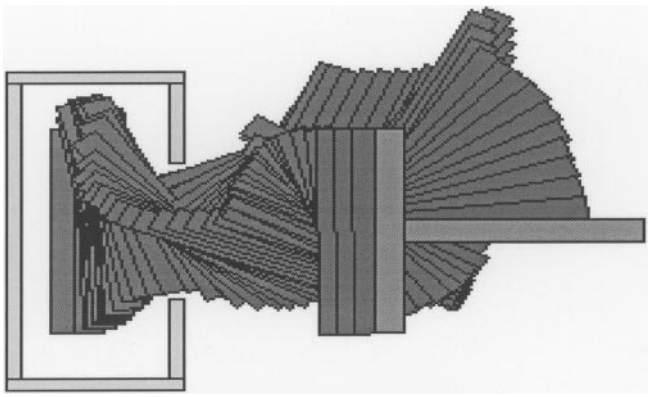


Fig. 13. Gross motion planning for T insertion.

planners[23] can plan motions for a complex shape in a relatively short time. This has motivated us to develop a compliant motion planner that uses a gross motion planner as a precursor. The approach is called skeleton refining.[5–7]

The traditional backprojection approach[7] assumes increasing uncertainty bounds with the travel distance, and this makes it difficult to find a motion sequence that guarantees the goal reachability. For a manipulator with a fixed base, however, the tool position error is bounded by the cumulative errors of the joint encoders, and is independent of the travel distance. Call this fixed error bound *Emax*. Given a motion planning problem, a gross motion planner is first used to plan robot motion assuming no uncertainty. If the clearance between the robot and obstacles are greater than $Emax|J|$ along the solution path, it can be executed without collisions ($|J|$ is norm of Jacobian). For the segments of the solution path where the clearance is smaller than $Emax|J|$, compliant motions need to be planned. We are currently developing an algorithm to convert a small-clearance path into a compliant motion strategy, which entails specifying the moving direction, compliant direction and motion termination condition.

One of the difficulties is that most collision-detection routines and distance-computation routines cannot reliably distinguish a contact (zero distance, feasible) and penetration (negative distance, impossible). Most gross motion planners consider a contact as a collision and cannot find a solution when a contact motion has to be used. In such cases, we shrink the moving object by a small amount to get an approximate solution. Fig. 13 shows a gross motion planned by the algorithm by Hwang and Chen[23], which took 3 seconds and 10,000 distance computations. Converting the approximate gross motion into a compliant motion is a major challenge; results are expected in the near future.

VII. CONCLUSION

To insert a complex shape using compliance, this paper presents a compliant control algorithm which is capable of rotating the object about a moving compliance frame at a contact point. A contact localization method for an object having a rectangular cross-section has been described. Furthermore, a moving compliance frame method using the location of the contact point in stiffness control loop for compliant insertion has been presented. To illustrate the

https://doi.org/10.1017/S0263574798000058 Published online by Cambridge University Press

performance of our algorithm, the task inserting a T into a C shape has been performed in a VME-bus based real time control system.

Two research problems can be proposed on the insertion of complex shapes. First, as mentioned in Section VI, a geometric algorithm for determining the feasibility of inserting a general concave 3-dimensional object using contact is required. Secondly, a method for localization of contact point needs to be developed for a general object whose geometric surface constraints ($\varphi(r)=0$ are semi-algebraic, i.e., intersections and unions of algebraic surfaces.

References

1. R. Paul and B. Shimano, "Compliance and control" *Proc. the Joint Automatic Control Conference*, ASME, San Francisco, California (1976) pp. 694–699.
2. J.K. Salisbury, "Active stiffness control of a manipulator in Cartesian coordinates" *Proc. of the 19th IEEE Conf. on Decision and Control*, Albuquerque, New Mexico (1980) pp. 95–100.
3. D.E. Whitney, "Force feedback control of manipulator fine motions" *ASME J. of Dynamic Systems, Measurement and Control*, **99**, No. 2, 91–97 (1977).
4. S. Lee and H. Asada, "Assembly of parts with irregular surface using active force sensing" *Proc. of the IEEE Int. Conf. on Robotics and Automation*, San Diego, California (1994) pp. 2635–2649.
5. T. Lozano-Perez, "The design of a mechanical assembly system" *Tech Report AI-TTR 397*, Artificial Intelligence Laboratory, MIT, Cambridge, MA, 1976).
6. R.H. Taylor, "Synthesis of manipulator control programs from task-level specification" *Ph.D. dissertation*, Dept. Computer Science, Stanford University, Stanford, CA 1976).
7. T. Lozano-Perez, M.T. Mason and R.H. Taylor, "Automatic synthesis of fine motion strategies for robotics" *Int. J. Robotics Research* **3**, No. 1, 3–24 (1984).
8. N. Hogan, "Impedance control: an approach to manipulation: part III–applications" *ASME Journal of Dynamic Systems, Measurement and Control* **107**, 17–24 (March, 1985).
9. A.A. Goldenberg and Peilin Song, "Analysis and design of position/force controllers Parts I, II" *Workshop 3 of IEEE Int. Conf. on Robotics and Automation: Force and Contact Control in Robotic Operation: Theory and Applications*, Minneapolis, Minnesota (1996) pp. 2.1–2.6.
10. M. Vukobratovic and D. Stokic, *Scientific Fundamental of Robotics 2: Control of Manipulation Robots, Theory and Application* (Springer-Verlag, Berlin, 1982).
11. H. Asada and S. Hirai, "Towards a symbolic-level force feedback: recognition of assembly process states" *Proc. of 5th Int. Symp. on Robotics Research*, Tokyo, Japan (1989) pp. 290–295.
12. D.R. Strip, "Insertions using geometric analysis and hybrid force-position control: Method and analysis" *Proc. of the IEEE Int. Conf. on Robotics and Automaion*, Philadelphia, Pennsylvania (1988) pp. 1744–1751.
13. P. Astuti and B.J. McCarragher, "Discrete event controller synthesis for the convergence of an assembly process" *Proc. of the IEEE Int. Conf. on Robotics and Automation*, Minneapolis, Minnesota (1996) pp. 1153–1158.
14. B.J. McCarragher, "The unsupervised learning of assembly using discrete event control" *Proc. of the IEEE Int. Conf. on Robotics and Automation*, Minneapolis, Minnesota (1996) pp. 1172–1177.
15. X. Zhou, Q. Shi and Zexiang Li, "Contact localization using force/torque measurements" *Proc. of the IEEE Int. Conf. on Robotics and Automation*, Minneapolis, Minnesota (1996) pp. 1339–1344.
16. T. Tsujimura and T. Yabuta, "Object detection by tactile sensing method employing force/torque information" *IEEE Trans. on Robotics and Automation* **5**, No. 4 444–450 (1989).
17. J.C. Latombe, A. Lazanas and S. Shekhar, "Robot motion planning with uncertainty in control and sensing" *Artificial Intelligence* **52**, 1–47 (1991).
18. J.F. Canny, "On computability of the fine motion plan" *Proc. of the IEEE Int. Conf. On Robotics and Automation, Scottsdale*, Arizona (1989) pp. 177–182.
19. M. Erdmann, "Using backprojection for the fine motion planning with uncertainty" *Int. J. Robotics Research* **5**, No. 1, 19–45 (1986).
20. R.C. Brost and A.D. Christiansen, "Probabilistic analysis of manipulation tasks: A computational framework" *Technical Report SAND92-2033* (Sandia National Laboratories, Albuquerque, NM, January 1994).
21. B.J. McCarragher, "Force Sensing from Human Demonstration: Stiffness, Impedance, and Kinesthetic Sensibility" *Proc. of the IEEE/RSJ Int. Conf. on Intelligent Robots and Systems*, Munich, Germany (1994) pp. 1226–1233.
22. W.S. Newman and M.E. Doring, "Augmented impedance control: an approach to compliant control of kinematically redundant manipulators" *Proc. of the IEEE Int. Conf. On Robotics and Automation*, Sacramento, California (1991) pp. 30–35.
23. Y.K. Hwang and P.C. Chen, "A complete and heuristic motion planner for the classical mover's problem" *Proc. of the IEEE Int. Conf. on Robotics and Automation*, San Diego, California, (1994) pp. 729–736.

https://doi.org/10.1017/S0263574798000058 Published online by Cambridge University Press